A study of sheared turbulence/shock interaction: velocity fluctuations and enstrophy behaviour

S. Jamme, M. Crespo and P. Chassaing

Abstract Direct Numerical Simulations of the idealized interaction of a normal shock wave with several turbulent shear flows are conducted. We analyse the behaviours of velocity and vorticity fluctuations and compare them to what happens in the isotropic situation. Investigation of the budgets of these quantities allows to isolate the mechanisms underlying the physics of the interaction, and reveals the importance of enthalpic production and baroclinic torque in such flows.

1 Introduction

The interaction of free isotropic turbulence with a normal shock wave has been the focus of several numerical studies in the past (see e.g. Lee *et al.* [3], Mahesh *et al.* [5]); and this subject is still a matter of concern in the scientific community (see e.g. Larsson and Lele [2]). In the above-mentioned works, Linear Interaction Analysis (LIA) and Direct Numerical Simulations (DNS) have been used to understand the main features of shock-turbulence interaction when the upstream turbulent flow is isotropic. Experimental investigations have also been conducted. However, the influence of anisotropy on the interaction has seldom been investigated. The purpose of the present work is to investigate how the presence of an idealized mean shear upstream of the shock may modify the interaction phenomenon compared to cases where no shear is present. In a previous paper (Jamme *et al.* [1]), we presented some DNS results explaining how thermodynamic fluctuations behave when a sheared turbulent flow interacts with a normal shock wave. We propose here to complete the picture of the flow by focusing on the behaviour of velocity and vorticity variances in such an interaction, and on the physical mechanisms responsible for this behaviour.

S. Jamme, M. Crespo and P. Chassaing
Université de Toulouse, ISAE, 10 avenue Edouard Belin, 31055 Toulouse, France
e-mail: stephane.jamme@isae.fr, matthieu.crespo@isae.fr, patrick.chassaing@isae.fr

2 Flow configuration and numerical method

We consider the interaction of a normal shock wave with a sheared turbulent flow involving a uniform (constant) mean velocity gradient and a non-uniform mean density (and temperature) gradient. The turbulent flow is no more homogeneous in the tranverse direction (x_2) of the shock wave (which was the case in the isotropic configuration). We solve the full three-dimensional Navier-Stokes equations in non-dimensional conservative form using a finite difference approach. The inviscid part is resolved using a fifth-order Weighted Essentially Non-Oscillatory scheme [7]. Viscous terms are computed using a sixth-order accurate compact scheme, and a third-order Runge Kutta algorithm is used to advance in time.

Equations are solved on a cubic domain of size 2π in the three directions (cf. figure 1) and a grid of 256x128x128 points is used. The mean flow is aligned with x_1. Periodic conditions are specified in the x_3 direction, and non-reflecting boundary conditions of Poinsot & Lele [6] along with a sponge layer are used for the top and bottom boundaries as well as for the outflow where the flow is subsonic. At the beginning of the calculation, a plane shock wave at Mach number M_1 is specified in the middle of the computational domain; the flow is steady on each side of the shock, satisfying the Rankine-Hugoniot relations.

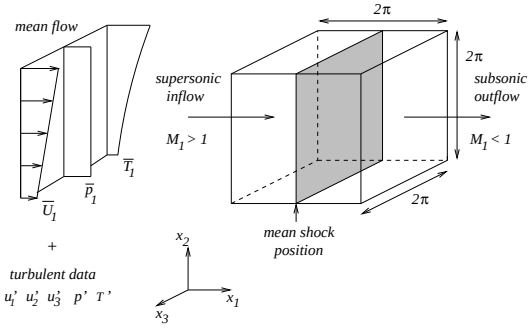

Fig. 1 Flow configuration.

At each time step, velocity, pressure, temperature, and density fields are specified at the inflow. These fields are superpositions of a supersonic mean flow and turbulent fluctuations (denoted further by a prime) in velocity, pressure, temperature, and density. The mean velocity at the inflow varies linearly across streamlines while the mean pressure is uniform. The mean temperature and density vary such as the mean Mach number is uniform :

$$\overline{U}_1(x_2) = U_0 + S(x_2 - x_{2\min}), \quad \overline{U}_2 = \overline{U}_3 = 0, \quad \overline{P}(x_2) = 1/(\gamma M_r^2), \quad \overline{T}(x_2) = M_r^2 \overline{U}_1^2 / M_1^2, \quad (1)$$

where the overbar denotes the conventional Reynolds average. The shear stress magnitude is controlled by the parameter S where $S = \partial \overline{U}_1 / \partial x_2$. Turbulent fluctu-

ations are then superposed onto the mean upstream flow and advected through the inflow boundary using Taylor's hypothesis. These turbulent data come from preliminary calculations of temporally evolving sheared turbulence so that the anisotropy of the velocity field used in the inflow plane is typical of a turbulent shear flow ($\widetilde{u_1''^2} > \widetilde{u_3''^2} > \widetilde{u_2''^2}$ and $\widetilde{u_1'' u_2''} \neq 0$). This inflow state slightly evolves in the first half of the computational domain, and the turbulence characteristics just before the shock are provided in table 1.

Table 1 Turbulence characteristics just before the shock wave (case STSI1)

$Re_\lambda = 27$	$\widetilde{u_1''^2}/q^2 = 0.352$	$\rho_{rms}/\overline{\rho} = 0.121$	$C_{\rho' u_1'} = -0.319$
$M_t = 0.159$	$\widetilde{u_2''^2}/q^2 = 0.299$	$p_{rms}/\overline{P} = 0.028$	$C_{\rho' u_2'} = 0.647$
$\chi = 0.031$	$\widetilde{u_3''^2}/q^2 = 0.349$	$T_{rms}/\overline{T} = 0.119$	$C_{T' u_1'} = 0.298$
$q^2/2 = 1.249$	$\widetilde{u_1'' u_2''}/q^2 = -0.127$	$C_{\rho' T'} = -0.873$	$C_{T' u_2'} = -0.649$

3 Results and discussion

A first DNS (STSI1) is conducted with the following values of the numerical parameters: $Re_r = \frac{\rho_r^* u_r^* l_r^*}{\mu_r^*} = 94$, $M_r = \frac{u_r^*}{c_r^*} = 0.1$, $Pr = 0.7$, where $(\cdot)_r^*$ refers to a dimensional reference variable. The mean Mach number is fixed to $M_1 = 1.5$, and the turbulence parameters in the inflow plane are the following : $Re_\lambda = Re_r \frac{\lambda u_{rms}}{\overline{\nu}} = 47$, $\frac{q^2}{2} = 1.5$, $M_t = \frac{q}{\overline{c}} = \frac{\sqrt{\overline{u_i' u_i'}}}{\overline{c}} = 0.173$. The mean velocity gradient equals $S = 1.5$, with $U_0 = 15$. The presence of a density and temperature gradient in the mean flow leads to non-isentropic thermodynamic fluctuations on both sides of the shock. Temperature and density fluctuations (entropy mode) dominate, and the entropy fluctuations are correlated with the velocity field such that the correlation between u_1' and T' is positive (see table 1). Three complementary DNS are also considered: they have the same parameters as STSI1, except that either u_1' and T' correlate negatively as in a compressible turbulent boundary layer ($C_{T' u_1'} = -0.462$) for case STSI2, or the mean Mach number is higher ($M = 3$) for case STSI3, or the mean shear is more important ($S = 6$) for case STSI4.

3.1 Velocity fluctuations

The turbulent kinetic energy is non-uniformly distributed on the normal Reynolds stresses. As in the isotropic situation, these quantities are first amplified across the shock wave, and then behave differently in the near field behind the shock : we observe a non-monotonic evolution of $\widetilde{u_1''^2}$, whereas the transverse normal Reynolds stresses decrease continuously (see figure 2a). This corresponds to the classical

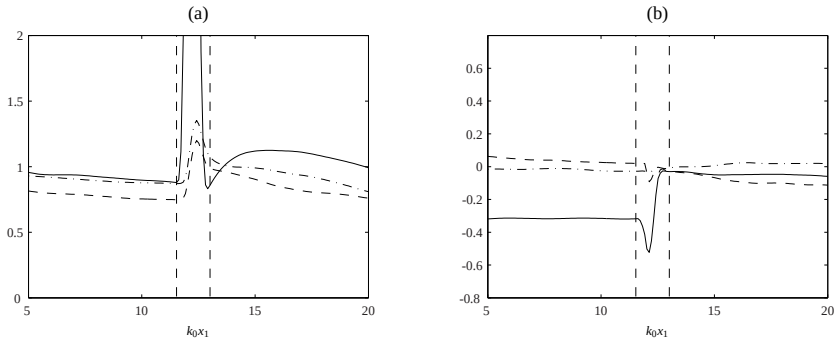

Fig. 2 STSI1: Streamwise evolution of the Reynolds stresses - $x_2 = L_2/2$. Normal components (a); (——) $\widetilde{u_1''^2}$; (– – –) $\widetilde{u_2''^2}$; (– · –) $\widetilde{u_3''^2}$. Off-diagonal components (b); (——) $\widetilde{u_1''u_2''}$; (– – –) $\widetilde{u_1''u_3''}$; (– · –) $\widetilde{u_2''u_3''}$.

transfer of energy between acoustical and vortical modes behind the shock and re-distribution of energy from $\widetilde{u_2''^2}$ and $\widetilde{u_3''^2}$ towards $\widetilde{u_1''^2}$. It can also be noticed that the turbulent kinetic energy is more amplified across the shock wave for case STSI2 than for case STSI1 (amplification factors of 1.58 and 1.21 respectively). The same influence of upstream entropy fluctuations with a negative correlation between u_1' and T' has been reported in the isotropic situation with a uniform mean upstream flow both by DNS and LIA: see Mahesh *et al.* [5].

A negative cross-correlation $\widetilde{u_1''u_2''}$ is also created in this flow as a consequence of the mean velocity shear. The budget of this quantity is given by equation (2).

$$\underbrace{\frac{3}{2}\frac{\overline{\rho}}{|\overline{\varepsilon}^\star|}\widetilde{U}_1\frac{\partial}{\partial x_1}\left(\widetilde{u_1''u_2''}\right)}_{(I)} = \underbrace{-\frac{3}{2}\frac{\overline{\rho}}{|\overline{\varepsilon}^\star|}\left(\widetilde{u_1''u_2''}\frac{\partial\widetilde{U}_1}{\partial x_1}\right)}_{(IIa)} \underbrace{-\frac{3}{2}\frac{\overline{\rho}}{|\overline{\varepsilon}^\star|}\left(\widetilde{u_2''^2}\frac{\partial\widetilde{U}_1}{\partial x_2}\right)}_{(IIb)} \underbrace{-\frac{3}{2|\overline{\varepsilon}^\star|}\left[\frac{\partial}{\partial x_1}\left(\overline{\rho}\widetilde{u_1''^2u_2''}\right)+\frac{\partial}{\partial x_2}\left(\overline{\rho}\widetilde{u_1''u_2''^2}\right)\right]}_{(III)}$$
$$\underbrace{-\frac{3}{2}\frac{\overline{u_2''}}{|\overline{\varepsilon}^\star|}\frac{\partial\overline{P}}{\partial x_1}}_{(IVa)} \underbrace{-\frac{3}{2|\overline{\varepsilon}^\star|}\left[\frac{\partial\left(\overline{p'u_2''}\right)}{\partial x_1}+\frac{\partial\left(\overline{p'u_1''}\right)}{\partial x_2}\right]}_{(IVb)} \underbrace{+\frac{3}{2}\frac{\Pi_{12}^d}{|\overline{\varepsilon}^\star|}}_{(IVd)} \underbrace{+\frac{3}{2}\frac{\overline{\varepsilon}_{12}^d}{|\overline{\varepsilon}^\star|}}_{(Vb)} \quad (2)$$

where: $\Pi_{ij} = \overline{p'\left(\frac{\partial u_i''}{\partial x_j}+\frac{\partial u_j''}{\partial x_i}\right)}$, $\Pi_d^\star = \overline{p'\left(\frac{\partial u_i''}{\partial x_i}\right)}$ (spherical part of Π_{ij}) and $\Pi_{ij}^d = \Pi_{ij} - \frac{2}{3}\Pi_d^\star\delta_{ij}$ (deviatoric part of Π_{ij}). Similarly, we have: $\overline{\varepsilon}_{ij} = \overline{u_j''\frac{\partial\tau_{ik}}{\partial x_k}} + \overline{u_i''\frac{\partial\tau_{jk}}{\partial x_k}}$, $\overline{\varepsilon}^\star = \overline{u_i''\frac{\partial\tau_{ik}}{\partial x_k}}$ (spherical part of $\overline{\varepsilon}_{ij}$) and $\overline{\varepsilon}_{ij}^d = \overline{\varepsilon}_{ij} - \frac{2}{3}\overline{\varepsilon}^\star\delta_{ij}$ (deviatoric part of $\overline{\varepsilon}_{ij}$).

Upstream of the shock wave, production by the mean shear (IIb) is balanced by the pressure-strain correlation (IVd), leading to a quasi-constant behaviour of $\widetilde{u_1''u_2''}$. We then notice a decrease of the magnitude of $\widetilde{u_1''u_2''}$ during the interaction with the shock (see figure 2b). We present in figure 3 the different terms of the budget equa-

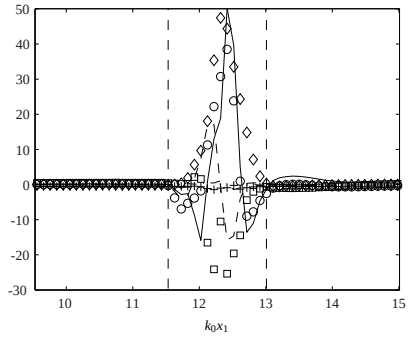

Fig. 3 STSI1 : budget of $\widetilde{u_1''u_2''}$ - $x_2 = L_2/2$. ($\circ\circ\circ\circ\circ$) (I); $(+++++)$ $(IIa+IIb)$; $(---)$ (III); ($\diamond\diamond\diamond\diamond\diamond$) (IVa); (——) (IVb); ($\square\square\square\square\square$) (IVd); $(-\cdot-\cdot-)$ (Vb).

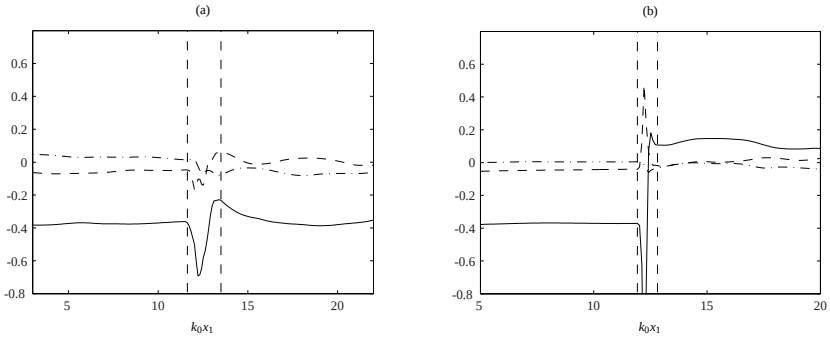

Fig. 4 Streamwise evolution of the off-diagonal components of the Reynolds stresses - $x_2 = L_2/2$. STSI2 (a); STSI3 (b). (——) $\widetilde{u_1''u_2''}$; $(---)$ $\widetilde{u_1''u_3''}$; $(-\cdot-)$ $\widetilde{u_2''u_3''}$.

tion (2) inside the shock zone (region where $\partial\overline{U}_1/\partial x_1 < 0$). All the terms of this budget are normalized by the absolute value of the dissipation, which allows to easily evaluate the importance of each term in comparison with viscous effects. Even if the statistics are clearly overestimated inside the shock zone because of the shock corrugations, it can however be concluded that the main "integral" contribution to the evolution of $\widetilde{u_1''u_2''}$ inside the shock thickness can be attributed to the action of enthalpic production (IVa). This is supported by the evolutions of $\widetilde{u_1''u_2''}$ for cases STSI2 and STSI3 (cf. figure 4) where enthalpic production is either lower (case STSI2) or greater (case STSI3) than in the reference case STSI1, which respectively leads to a smaller or higher effect on the cross-correlation $\widetilde{u_1''u_2''}$ during the interaction with the shock wave. This result is in contradiction with the RDT conclusions of Mahesh *et al.* [4] who assigned the tendency of $\widetilde{u_1''u_2''}$ to decrease upon normal compression to an amplification of the pressure-strain correlation (IVd) and the consequent upsetting of the initial balance between production and the pressure strain correlation in the shear flow. It should also be noticed that, since the intensity of the enthalpic production depends on the mean pressure gradient across the shock and also on the turbulent mass fluxes that are generated in this flow (due to the simultaneous pres-

ence of a mean shear for the velocity and the density), the production mechanisms of the thermodynamic fluctuations described in Jamme *et al.* [1] are closely linked to the behaviour of $\widetilde{u_1''u_2''}$ during the interaction. Finally, downstream of the shock, the flow reorganises itself since the new level of $\widetilde{u_1''u_2''}$ is not consistent with the value of the mean shear after the interaction ($S_{downstream} < S_{upstream}$).

3.2 Vorticity fluctuations

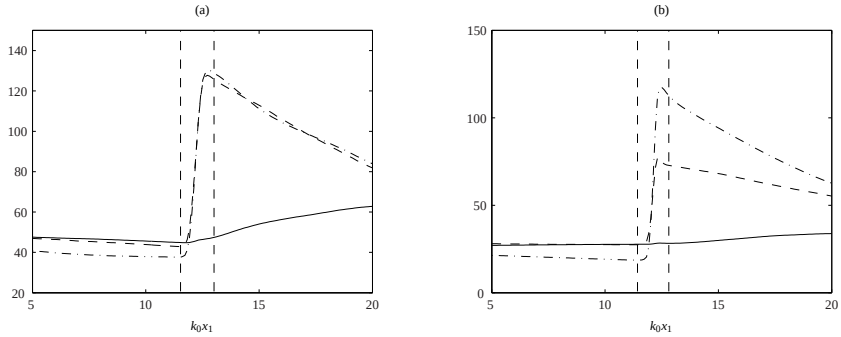

Fig. 5 Streamwise evolution of the vorticity variances - $x_2 = L_2/2$. STSI1 (a); STSI4 (b). (——) $\overline{\omega_1'^2}$; (– – –) $\overline{\omega_2'^2}$; (– · –) $\overline{\omega_3'^2}$.

Figure 5 shows that the global behaviour of vorticity variances is similar to the one observed in isotropic turbulence/shock interaction cases : outside the shock zone, viscous dissipation (*VIII*) is in competition with turbulent vortex stretching (*III*) [see bugdet equation (3) for the analytical expression of the different terms]. These terms are nearly balanced upstream of the shock, leading to a quasi-constant evolution of the vorticity variances, whereas downstream of the shock, dissipation overwhelms stretching for the transverse vorticity variances only, leading to a clear decrease of these quantities. Then, across the shock wave, the transverse components are clearly amplified while the streamwise component remains nearly unaffected. Inside the shock zone, mean vortex stretching (*II*) balances mean compression (*IV*) for $\overline{\omega_1'^2}$ only, as in the isotropic situation. However, as reported in table 2, $\overline{\omega_3'^2}$ appears more amplified than $\overline{\omega_2'^2}$ in the sheared configurations. Figure 6 shows that this behaviour can be attributed to the action of the baroclinic term inside the shock zone that is more intense for $\overline{\omega_3'^2}$ than for $\overline{\omega_2'^2}$. For $\overline{\omega_3'^2}$, the baroclinic torque can be written: $2\overline{\frac{1}{\rho^2}\omega_3'\frac{\partial\rho}{\partial x_1}\frac{\partial P}{\partial x_2}} - 2\overline{\frac{1}{\rho^2}\omega_3'\frac{\partial\rho}{\partial x_2}\frac{\partial P}{\partial x_1}}$, which involves the product of $\frac{\partial P}{\partial x_1}$ and $\frac{\partial\rho}{\partial x_2}$ that are clearly non-negligible inside the shock zone. Moreover, for a given shock intensity, this term is all the more important that the mean density gradient along x_2 is pronounced. This explains why the difference in the amplifications of $\overline{\omega_2'^2}$ and $\overline{\omega_3'^2}$ is greater for case STSI4 than for case STSI1 (see figure 5b).

Table 2 Amplification factors of the vorticity variances for different cases ($x_2 = L_2/2$).

Amplification of	LIA ($M_1 = 1.5$)	isotropic DNS ($M_1 = 1.5$)	STSI1	STSI4
$\overline{\omega_1'^2}$	1	1.1	1.05	1.02
$\overline{\omega_2'^2}$	3.21	2.83	2.95	2.63
$\overline{\omega_3'^2}$	3.21	2.83	3.44	5.61

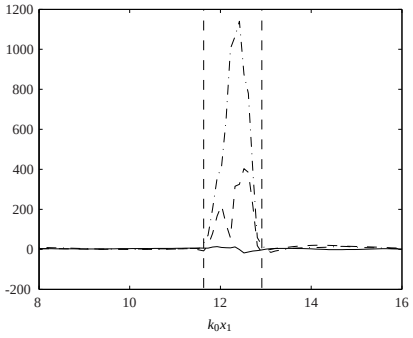

Fig. 6 STSI1 - $x_2 = L_2/2$. Comparison of the baroclinic torque (VI) in the budget equations of $\overline{\omega_1'^2}$ (——); $\overline{\omega_2'^2}$ $(- - -)$ and $\overline{\omega_3'^2}$ $(- \cdot -)$.

$$\underbrace{\overline{U}_j \frac{\partial \overline{\omega'_\alpha \omega'_\alpha}}{\partial x_j}}_{(I)} = \underbrace{2\overline{\omega'_\alpha \omega'_j} \overline{s}_{\alpha j}}_{(II)} + \underbrace{2\overline{\omega'_\alpha \omega'_j s'_{\alpha j}}}_{(III)} - \underbrace{2\overline{\omega'_\alpha \omega'_\alpha} \overline{s}_{jj}}_{(IV)} - \underbrace{\overline{\omega'_\alpha \omega'_\alpha s'_{jj}}}_{(V)} + \underbrace{2\varepsilon_{\alpha jk} \overline{\frac{1}{\rho^2} \omega'_\alpha \frac{\partial \rho}{\partial x_j} \frac{\partial P}{\partial x_k}}}_{(VI)}$$
$$\underbrace{- \frac{\partial \left(\overline{\omega'_\alpha \omega'_\alpha u'_k} \right)}{\partial x_k}}_{(VII)} \underbrace{+ 2\varepsilon_{\alpha jk} \overline{\omega'_\alpha \frac{\partial}{\partial x_j} \left(\frac{1}{\rho} \frac{\partial \tau_{kq}}{\partial x_q} \right)}}_{(VIII)} \quad (3)$$

with: $s_{ij} = \frac{1}{2} \left(\frac{\partial u_i}{\partial x_j} + \frac{\partial u_j}{\partial x_i} \right)$, and ε_{ijk} stands for the permutation tensor (no summation on α).

References

1. Jamme, S., Crespo, M., Chassaing, P.: Thermodynamic fluctuations behaviour during a sheared turbulence/shock interaction. In Turbulence and Interactions, proceedings of the TI 2009 conference. Notes on Numerical Fluid Mechanics and Multidisciplinary Design **110** (2010).
2. Larsson, J., Lele, S.K.: Direct numerical simulation of canonical shock/turbulence interaction. Phys. Fluids **21**, 126101 (2009).
3. Lee, S., Lele, S.K., Moin, P.: Interaction of isotropic turbulence with shock waves: effect of shock strength. J. Fluid Mech. **340**, 225-247 (1997).
4. Mahesh, K., Lele, S.K., Moin, P.: The response of anisotropic turbulence to rapid homogeneous one-dimensional compression. Phys. Fluids **6**, 1052-1062 (1993).
5. Mahesh, K., Lele, S.K., Moin, P.: The influence of entropy fluctuations on the interaction of turbulence with a shock wave. J. Fluid Mech. **334**, 353-379 (1997).
6. Poinsot, T.J., Lele, S.K.: Boundary conditions for direct simulations of compressible viscous reacting flows. J. Comp. Phys. **101**, 104-129 (1992).
7. Ponziani, D., Pirozzoli, S., Grasso, F.: Development of optimized Weighted-ENO schemes for multiscale compressible flows Int. J. Numer. Meth. in Fluids **42**, 953-977 (2003).